

Identifying non-invasible habitats for marine copepods using temperature-dependent R_0

Harshana Rajakaruna · Carly Strasser · Mark Lewis

Received: 28 October 2010 / Accepted: 9 September 2011 / Published online: 23 September 2011
© Springer Science+Business Media B.V. 2011

Abstract If a non-indigenous species is to thrive and become invasive it must first persist under its new set of environmental conditions. Net reproductive rate (R_0) represents the average number of female offspring produced by a female over its lifetime, and has been used as a metric of population persistence. We modeled R_0 as a function of ambient water temperature (T) for the invasive marine calanoid copepod *Pseudodiaptomus marinus*, which is introduced to west coast of North America from East Asia by ship ballast water. The model was based on temperature-dependent stage-structured population dynamics given by a system of ordinary differential equations. We proposed a methodology to identify habitats that are non-invasible for *P. marinus* using the threshold of $R_0(T) < 1$ in order to identify potentially invasible habitats. We parameterized the model using published data on *P. marinus* and applied $R_0(T)$ to identify the range of non-invasible habitats in a global scale based

on sea surface temperature data. The model predictions matched the field evidence of species occurrences well.

Keywords Net reproductive rate · Invasive species · Marine copepods · *Pseudodiaptomus marinus* · Temperature · Stage-structured population models · Ordinary differential equations · Ecological modeling · Habitat invasibility · Habitat suitability

Introduction

Assessment of habitat invasibility often relies on statistical matching of the external environmental variables in native and novel habitats via methods such as ecological niche modeling (ENM) (Jeschke and Strayer 2008; Mercado-Silva et al. 2006). However, it is often the case that invasive species can tolerate environmental conditions in novel habitats that are outside those found in their native habitats (Broennimann et al. 2007; Elith and Leathwick 2009). This indicates that the absence of a species in particular environments may not necessarily mean such environments are unsuitable for the species. As an alternative to ENM, we can determine the response of potential invaders to specific environmental conditions under controlled laboratory settings. For example, we can measure the rates of mortality, offspring production, and stage durations under different environmental conditions. However, we must still translate these

H. Rajakaruna (✉) · M. Lewis
Centre for Mathematical Biology,
Department of Biological Sciences,
University of Alberta, Edmonton, AB, Canada
e-mail: rajakaru@ualberta.ca

C. Strasser · M. Lewis
Department of Mathematical and Statistical Sciences,
University of Alberta, Edmonton, AB, Canada

C. Strasser
Department of Oceanography, Dalhousie University,
Halifax, NS, Canada

measures into a habitat invisibility indicator or metric. Will a population persist and grow under a given set of environmental conditions? To answer this question we can use the net reproductive rate R_0 of a population as a metric. R_0 is a measure of a population's reproductive success (Ackleha and de Leenheer 2008), and therefore, is a population fitness trait, which represents the average number of offspring produced by a female over its lifetime (de-Camino-Beck and Lewis 2008). It has been used in evolutionary invasion analysis to predict long term evolutionary outcomes (Hurford et al. 2010). When $R_0 > 1$, a population grows, and when $R_0 < 1$, a population tends to decrease to extinction (Boldin 2006). Thus, we can use R_0 to decide which habitats are suitable or unsuitable for a species by determining whether environmental parameters result in $R_0 > 1$ or $R_0 < 1$. We derived R_0 from a mechanistic state-structured population model given by a system of ordinary differential equations and parameterized by data from laboratory experiments. This method allows us to predict the range of habitats that are *non-invasible* or *potentially invasible* for a species or strain.

Our model species, *Pseudodiaptomus marinus*, is an invasive marine calanoid copepod that was introduced to the Pacific coast of North America (Fleminger and Kramer 1989) and coastal waters in Southern Chile from its native habitat in East Asia via ballast water (Bolens et al. 2002). It is a perennial egg-carrying calanoid copepod, spawns continuously throughout the year, and has multiple overlapping generations (Uye et al. 1983). Its life-history traits such as fertility, mortality and maturation rates are known to be functions of temperature (Liang and Uye 1997a; Uye et al. 1983). *P. marinus* has also been reported in many other oceanic habitats around the world (Razouls et al. 2011) and has been expanding its range (Jiménez-Pérez and Castro-Longoria 2006). Despite high propagule pressure, *P. marinus* has not been reported in the coastal ecosystems of Oregon and Washington (Cordell et al. 2008), or Vancouver Harbour (Piercey et al. 2000), indicating that it may be a successful invader only in selected habitats. It has not been clear what environmental factors limit its geographical distribution in terms of its physiological tolerance.

Here we modeled R_0 of *P. marinus* as a function of temperature assuming continuous time stage-structured population dynamics of the species based

on a system of linear first order ordinary differential equations (ODEs). ODE transmission models in epidemiology literature are commonly evaluated using R_0 , although it is less commonly used in stage-structured life-history dynamics. We parameterized the model using previously published data from laboratory experiments and field surveys (Liang and Uye 1997a; Uye et al. 1983).

The R_0 -based approach to determining habitat invasibility, while appealing, is necessarily limited by the range of environmental conditions under which the laboratory experiments can produce parameters. When R_0 is calculated using model parameters that were estimated for a limited range of primary environmental variables (e.g. temperature only), with other secondary environmental variables (e.g. salinity, day-light levels) held at optimal levels in the laboratory, results are not likely to be representative of what the species experiences in the field. In these cases, however, it is possible to use the R_0 -based approach to identify which habitats are non-invasible. If $R_0 < 1$ when secondary variables are optimal it also should remain below one when secondary variables are suboptimal. In this way we can identify temperature (T) thresholds for invisibility of the marine copepod *P. marinus* using $R_0(T)$.

The method we develop yields $R_0(T)$ as a function of temperature, allowing us to predict the range of temperatures that inhibit the growth of *P. marinus*, and thereby to predict the range of habitats that are potentially invasible to *P. marinus*. This method can be generally applied to model R_0 for other similar species. The results is complimentary to ENM and has a further advantage over ENM in terms of predicting species' potential spread over habitats that differ from their native habitats.

Methods

We modeled stage-structured population dynamics of *P. marinus* using a system of first order linear ODEs assuming continuous year-round growth and overlapping generations (Uye et al. 1983). We followed the methods in van den Driessche and Watmough (2002) to model the net reproductive rate R_0 based on the ODE model. Our model contains fertility, maturation, and mortality rate parameters. Because stage based fertility, mortality, and maturation rates are

temperature-dependent (Uye et al. 1983; Liang and Uye 1997a), we modeled the rate parameters as functions of temperature. This allowed us to calculate the temperature-dependent R_0 .

Model

Egg-carrying marine calanoid copepod *Pseudodiaptomus marinus* has six naupliar stages, five copepodid stages, and one adult stage. We do not include naupliar stage 1 in the model as data corresponding to this stage are not available due to difficulty in measurement as it lasts only few minutes (Uye et al. 1983). However, the data on naupliar stage 2 can be considered as an approximation, combining stage 1 and stage 2 into a single stage.

We define $n(t)$ to be a vector representing the stage composition of the population at time t , and $A(T)$ be a matrix of parameter space of vital rates (fertility, maturation, and mortality) that depend on temperature (T). Thus, we can write the rate of change of stage composition as follows:

$$\frac{dn(t)}{dt} = A(T)n(t) \tag{1}$$

where,

$$n(t) = [n_1(t), n_2(t), \dots, n_{12}(t)]^T$$

$$A(T) = \begin{pmatrix} -\mu_1(T) - \gamma_1(T) & 0 & : & 0 & q\beta(T) \\ \gamma_1(T) & -\mu_2(T) - \gamma_2(T) & : & 0 & 0 \\ 0 & \gamma_2(T) & : & : & : \\ : & : & : & -\mu_{11}(T) - \gamma_{11}(T) & 0 \\ 0 & 0 & : & \gamma_{11}(T) & -\mu_{12}(T) \end{pmatrix}$$

where, $\mu_i(T)$ and $\gamma_i(T)$, $\beta(T)$ are stage-dependent mortality, maturation, and fertility rates respectively, which are functions of temperature. Here, n_1 represents the number of eggs, n_2, \dots, n_6 represents the number of individuals in the five naupliar stages (excluding stage 1), n_7, \dots, n_{12} represents the number of individuals in the five copepodid stages and the adult stage 12. $\beta(T)$ is the fertility rate (rate of egg production) in adult females as a functions of temperature. The constant q is the average proportion of

ovigerous females in the adult population, which is estimated to be 0.61 (Liang and Uye 1997b). See Table 1 for all notations. We derived the net reproductive rate R_0 for *P. marinus* based on the above model as described below.

R_0 as a function of temperature

First, we wrote the matrix A as $A = F - V$ where F is the matrix of fertility coefficients (non-negative and non-zero), and V is the matrix of transition coefficients (i.e. net maturation and mortality rates). R_0 can then be written as $R_0 = \rho[FV^{-1}]$, where ρ is the spectral radius of the matrix FV^{-1} (van den Driessche and Watmough 2002). That is $\rho[FV^{-1}] = \max_{1 \leq i \leq n} |\lambda_i|$ where $\lambda_1, \lambda_2, \dots, \lambda_n$ are eigenvalues of the square matrix FV^{-1} . Note that the intrinsic growth rate defined as the maximum real eigenvalue of the square matrix A has a non-linear relationship with net reproductive rate R_0 (Wallinga and Lipsitch 2007). However, the intrinsic growth rate is positive if and only if $R_0 > 1$.

We modified the model to express R_0 as a function of temperature, such that $R_0(T) = \rho[F(T)V(T)^{-1}]$. Using the graph reduction method (de-Camino-Beck and Lewis 2007) (see derivation in ‘‘Appendix 1’’), we can also write R_0 as,

$$R_0(T) = \frac{\text{rate of production of offspring by females}}{\text{mortality rate at stage } s} \prod_{i=1}^{s-1} \left(\frac{\gamma_i(T)}{\mu_i(T) + \gamma_i(T)} \right)$$

$\underbrace{q\beta(T)}_{\text{rate of production of offspring by females}}$
 $\underbrace{\mu_s(T)}_{\text{mortality rate at stage } s}$

where s is the final stage (stage 12) for *P. marinus*. We modeled temperature-dependent parameters in the model as described in the next section.

Table 1 Meaning of mathematical notations

Notation	Description
n_1	Number of eggs
n_2, \dots, n_6	Number of individuals in the five naupliar stages (excluding stage I)
n_7, \dots, n_{12}	Number of individuals in the five copepodid stages and the adult stage 12
$\beta(T)$	Fertility rate (rate of egg production) in adult females as a function of temperature
q	Average proportion of ovigerous females in the adult population, assumed to be a constant value of 0.61 (Liang and Uye 1997b)
$\mu_i(T)$	Rate of mortality in stage i as a function of temperature
$\gamma_i(T)$	Rate of maturation of individuals surviving to stage i as a function of temperature
A	12×12 linear matrix composed of maturation, mortality and fertility rates, such that $dn(t)/dt = An(t)$, where n are vectors of stage classes
T	Temperature
R_0	Net reproductive rate
f_m	Maximum rate of fertility
f_l	Fertility at the lowest temperature
w	Shape parameter that accounts for the depression in fertility rate at low temperatures
b	Lag parameter to relax the assumption that the fertility rate curve otherwise intercepts y-axis at the origin
$z_a(t)$	Proportion of individuals at each stage a
d_a	Stage (a) duration times random variable
\bar{d}_a	Mean stage (a) duration times
D_a	Stage (a) development time distribution
\bar{D}_a	Mean stage (a) development times
α_a	Constant that varies with stage a in maturation function of temperature $\gamma_a(T) = (T - 1)^{1.8}/(\alpha_a - \alpha_{a-1})$ where $\alpha_0 = 0$ derived from Belehradek's function
ϕ	Scale parameter in $Sv = \exp(-\phi a^\chi)$
χ	Shape parameter in $Sv = \exp(-\phi a^\chi)$
κ	Parameters from mortality as a quadratic function of temperature $\mu(T) = \kappa_2 T^2 + \kappa_1 T + \kappa_0$

Fertility rates $\beta(T)$

Eggs are produced by adult females in stage 12 (n_{12}). Fertility rate, $\beta(T)$, can be written as $\beta(T) = f(T)/\Delta t$, where $f(T)$ is the number of eggs produced by an adult female over time Δt at average temperature T . Uye et al. (1983) fitted a linear model to parameterize $\beta(T)$. The linear model takes the form $\beta(T) = 0.771T - 4.48$, with $R^2 = 0.84$. Residual analyses of Uye's data, however, show that residuals are not randomly distributed along the fitted line indicating that linearity may not be the appropriate assumption. There is a depression in fertility rates at low temperatures. Furthermore, the linear model assumes that fertility is unbounded with increasing temperature, which is not biologically valid. We therefore refitted the data with a sigmoidal curve, assuming log normally distributed errors. We incorporated a lag parameter

(b) to relax the assumption that the curve must otherwise intercept the y-axis at the origin. The sigmoidal curve allows us to assume that fertility rate has a maximum value. Biologically it is more appropriate to assume that fertility rate is a bell-shaped curve, however we did not have the data to extend our curve to the point where $\beta(T)$ begins to decrease at high temperatures. Hence, our model for fertility rate can be written as,

$$\beta(T) = f_m f_l e^{w(T-b)} / [f_m + f_l (e^{w(T-b)} - 1)]$$

where, f_m is the maximum rate of fertility, f_l is fertility rate at the lowest temperature, and w is a shape parameter that accounts for the depression in fertility at lower temperatures. We compared the regression fit of linear model used in Uye et al. (1983) with our sigmoidal model using residual sum of squares.

Maturation rates $\gamma_i(T)$

We solved the system of ODE’s represented by Eq. 1 analytically for initial values corresponding to a single individual in stage 1, $n_1(0) = 1$, and $n_i(0) = 0$ for $i = 2, \dots, 12$. This allowed us to follow a single cohort over time with no additional individuals being added to the system (“Appendix 2”).

In experimental studies, maturation rates are commonly calculated using median development times, or the time it takes for 50% of the cohort to mature from eggs past a given stage (e.g. Uye et al. 1983; Breteler et al. 1994; Lee et al. 2003.). An assumption underlying such conventional calculation of maturation rate using ‘proportions not yet past given stage’ is that daily mortality rates of copepods are the same across all stages for a cohort. It excludes the mortality rate parameter from the equation and assumes that daily stage proportions are the result of individuals maturing from one stage to another. We made the same assumption here in the estimation of maturation rates from our model as *P. marinus* data are available only as proportions of a cohort remains in each stage over time with the same assumption. Thus, we normalized the stage size data $n_a(t)$ for each time step (t) dividing it by total remaining population of the cohort at that time step to give the proportion at each stage $z_a(t)$. This assumption made the proportion at each stage $z_a(t)$ to be independent from the mortality rates (“Appendix 3”).

Using Eq. 6 in “Appendix 3” we can describe the proportion of individuals not having past stage a , i.e. $\sum_{i=1}^a z_i(t)$, as,

$$\sum_{i=1}^a z_i(t) = 1 - \sum_{i=1}^a \left[\prod_{\substack{j=1 \\ j \neq i}}^a \frac{\gamma_j}{\gamma_j - \gamma_i} (1 - e^{-\gamma_i t}) \right]. \quad (2)$$

As shown by Cox (1967), this equation can also be derived from assuming the length of time that a copepod takes in a stage (stage duration time) as an exponentially distributed random variable, d_a , such that the probability density function of d_a is $\gamma_a e^{-\gamma_a t}$ and cumulative density function of d_a is $(1 - e^{-\gamma_a t})$, where γ_a is the stage maturation rate, and $\mu_a = 0$ for all stages a . The length of mean time taken to exit stage a , i.e. stage development time, D_a , becomes a random variable defined as $D_a = \sum_{i=1}^a d_i$ of which the cumulative density function of is $[1 - \sum_{i=1}^a z_i(t)]$. The

quantity $\sum_{i=1}^a z_i(t)$, thus yields the proportion of individuals not having past stage a .

We fitted stage proportion data from Uye et al. (1983) to Eq. 2 using nonlinear least squares regression to estimate γ_a . The data used were collected for *P. marinus* at 20°C. We calculated the mean stage duration times d_a as $\bar{d}_a = \frac{1}{\gamma_a}$ at 20°C. This yielded from the fact that d_a is an exponentially distributed random variable. We then used d_a calculated for 20°C to estimate the relationship between D_a and temperature (T). We assumed the relationship given by Behlradek’s function, $\bar{D}_a = \alpha_a(T - 1)^{-1.8}$ (as used by Uye et al. (1983) for *P. marinus*), where T is temperature in centigrade and α_a is a constant that varies with stage a . Using calculated α_a , we estimated the parameters for $\gamma_a(T)$ from the following equation derived from the above, $\gamma_a(T) = (T - 1)^{1.8} / (\alpha_a - \alpha_{a-1})$ for each stage a at temperatures (T). Here, $\alpha_0 = 0$.

As an advancement to the above model, we modified Eq. 1 to assume that stage duration times are gamma distributed (Breteler et al. 1994; Lee et al. 2003) by replacing the earlier assumption on exponentially distributed times. That is, probability density function of d_a now becomes $\frac{\gamma_a^k}{\Gamma(k)} t^{k-1} e^{-\gamma_a t}$ where, $\Gamma(k) = (k - 1)!$, $\gamma_a > 0$, $k > 0$. Mathematically this can be achieved by assuming that there are sub-stages (k_a) within each stage a in Eq. 1 given that duration times of sub-stages are exponentially distributed (see Linear Chain Trick in MacDonald 1978 for a full description). Here we assumed that mortality and maturation rates of sub-stages were the same for each stage. Thus the number of sub-stages, k , in Eq. 1 is equivalent to assuming the shape parameter k in the gamma distributed stage duration times. Here we assumed k_a to be the same k for all stages a as previous studies suggested for copepods (e.g. Breteler et al. 1994; Lee et al. 2003). The method for fitting the model with multiple sub-stages is outlined in “Appendix 4”.

The mean stage duration times d_a become $\bar{d}_a = \frac{k}{\gamma_a}$ for the modified model for gamma distributed d_a . Therefore

$$\gamma_a(T) = k(T - 1)^{1.8} / (\alpha_a - \alpha_{a-1}) \quad (3)$$

where $\alpha_0 = 0$. Note that the advanced model (see “Appendix 4” through Eq. 3) reduces to the simple model when $k = 1$ and $\varepsilon = 0$. We compared the model fits for $k = 1$, and $k = 2, 3$ using AIC and χ^2

test to determine which model assumption was the best to estimate $\gamma_a(T)$. We used the estimated stage duration times to calculate mortality rates as shown in the next section.

Mortality rates $\mu(T)$

Liang and Uye (1997a) estimated the percent survival of nine generations of the population for *P. marinus* from the west coast of Japan under different mean temperatures. We used these data to estimate survival curves at different temperatures. Because of their estimation procedure, Liang and Uye reported percent survival >100% in some cases; these values were reduced to 100%. We fitted the function $Sv = \exp(-\phi a^\chi)$ for the proportion surviving from eggs to stage a , where ϕ is a scale parameter and χ is a shape parameter. We estimated ϕ and χ using non-linear least squares regression. We calculated the proportion of individuals that died in each stage with respect to the proportion of individuals that matured into the current stage from the previous stage using Sv . We refer to Sv as a modified Weibull function because $(1 - Sv)$ is the cumulative density function of the Weibull distribution (1951).

To obtain estimates of mortality rates $\mu_a(T)$ for each stage a , we divided the estimated proportions that died in each stage by the stage duration times, given by $d_a = \frac{1}{\gamma_a}$ for the exponential distributions (simple model), and $d_a = \frac{k}{\gamma_a}$ for gamma distributions (advanced model) at the same temperatures. We pooled mortality rates across stages so as to be consistent with our earlier assumption (in modeling stage maturation rates using experimental data) that mortality rates across all stages are the same. We fitted a quadratic function $\mu(T) = \kappa_2 T^2 + \kappa_1 T + \kappa_0$ for the pooled data using nonlinear least squares regression. We did not use the survey measurement data at 27.4°C in Uye et al. (1983) for above calculations as it yielded near zero daily mortality rates at such a comparatively high temperature which resulted in a biologically inexplicable pattern that contradicted the general trend, suggesting that those data may be outliers.

We tested whether the assumption behind pooling data, i.e. mortality rates are the same across all stages for a given temperature (as in Breteler et al. 1994; Uye

et al. 1983) is a valid assumption for this species. To do this, we used the method of positioning means within confidence intervals (Venables and Ripley 2002).

Now we had $\beta(T)$, $\gamma_a(T)$ and $\mu(T)$ modeled exclusively as functions of temperature to finally fit into $R_0(T)$ model.

The model for $R_0(T)$ for any k is as follows

$$R_0(T) = \frac{q\beta(T)}{\mu_s(T)} \prod_{i=1}^{s-1} \left(\frac{\gamma_i(T)}{\mu_i(T) + \gamma_i(T)} \right)^k \quad (4)$$

(see derivation in “Appendix 1”).

Application and validation

We used the parameterized $R_0(T)$ to predict the range of habitats that are non-invasible to *P. marinus* on a global scale, based on sea surface temperature data from NOAA Optimum Interpolation (OI) SST V2. The range of habitat temperatures where $R_0(T) < 1$ is considered to be non-suitable for population persistence and hence non-invasible. We compared our predictions with the known occurrences of *P. marinus*.

Results

Fertility rates

We found that the sigmoidal model for fertility rates fits the data better than the linear model (Fig. 1). The residual sum of squares (RSS) for the sigmoidal model was 97.37, compared to 126.08 for the linear model. Parameters for the sigmoidal model were $f_m = 13.89$, $f_l = 0.61$, $w = 0.35$, $b = 6.01^\circ\text{C}$. Using the sigmoidal model, fertility rates started at zero near or slightly above 0°C , and tended to reach a maximum at temperatures above 25°C . Intuitively, fertility rate should peak at some optimal temperature, then decrease with increasing temperatures, which our sigmoidal model does not recreate. However, we are more interested in predicting dynamics at lower temperatures, so the sigmoidal model is sufficient. The results indicate that sigmoidal model is a better statistical approximation as well as having a theoretically better rationale than the linear model.

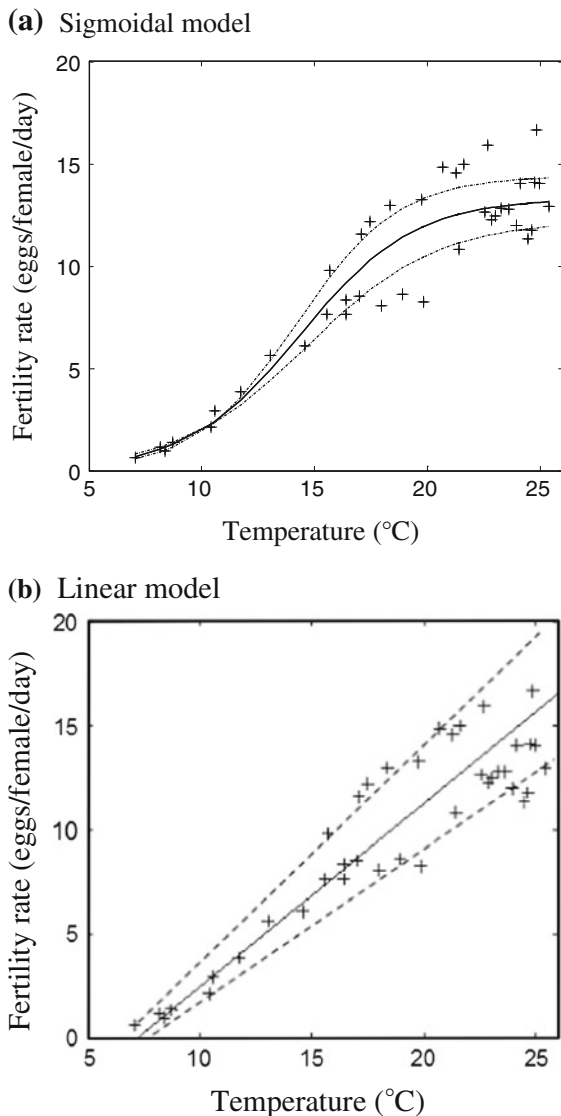


Fig. 1 Rate of fertility of adult females at different temperatures comparing sigmoidal model with linear model by Uye et al. (1983). Dashed lines indicate 95% CI

Maturation rates

We estimated stage maturation rates for cases $k = 1, 2,$ and 3 by fitting Eq. 2 and its advanced model (in “Appendix 4”) to data from Uye et al. (1983) at 20°C (Fig. 2). We compared the fits using AIC and found that $k = 3$ is the better statistical model than $k = 1, 2$ (Table 2). The model with $k = 3$ gives the lowest AIC (Table 2). Note that P values for χ^2 goodness of fit test for $k = 1$ and $k = 2$ with respect to $k = 3$ was <0.001 . This suggests that model with $k = 3$ is significantly

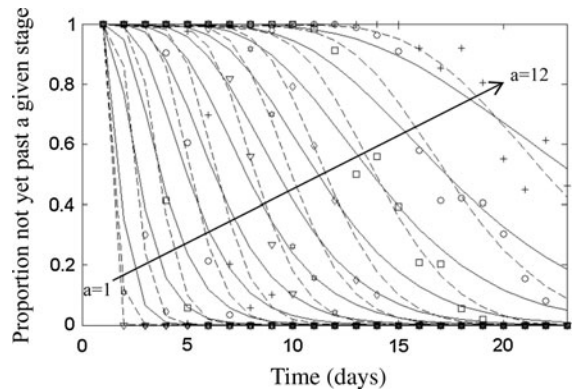


Fig. 2 Proportion of individuals in the population not yet past a given stage a (at 20°C) obtained by fitting Eq. 2 to data from Uye et al. (1983). Solid lines are the fits for $k = 1$, dashed lines are the fits for $k = 3$

different from models with $k = 1$ and $k = 2$. Hence, we concluded that the model with $k = 3$ is the most reasonable. The estimated temperature-independent α values in Eq. 3 are given in Table 3. We used them to calculate stage-maturation rates and duration times at any temperatures from Eq. 3

Mortality rates

We estimated values of ϕ and χ for Weibull model for different generations at different temperature regimes (Fig. 3, Table 4). The parameters estimated for the stage-independent mortality rates as a quadratic function of temperature were $\kappa_2 = 0.0022/\text{day}$, $\kappa_1 = -0.0563/^{\circ}\text{C day}$, $\kappa_0 = 0.4211/^{\circ}\text{C}^2 \text{ day}$ (Fig. 4). The assumption that mortality rates are the same across all stages was tested by examining the confidence intervals of estimates in each stage-based mortality rate function of temperature. The mean values of the model coefficients fell within the confidence intervals of every other stages indicating that the data can be pooled. Hence, our assumption that mortality rates are the same across all stages for a given temperature is valid for *P. marinus*.

Net reproductive rate

We plotted $R_0(T)$ after incorporating the parameterized sub-models $\beta(T)$, $\gamma_a(T)$ and $\mu(T)$ (Fig. 5). $R_0(T)$ tends to curve downwards at high temperatures due to increasing mortality rate (Fig. 4) that suppresses the positive effect of increasing fertility rates at higher temperatures (Fig. 1).

Table 2 Model comparisons for cases $k = 1, 2,$ and 3 in Eq. 2 and its advanced model (in “Appendix 4”)

Model	RSS	LL	(LL/LLmax)	χ^2	Degree	AIC	Δ AIC	$P(\chi)^2$
$k = 3$	0.57	120.56	0.00	0.00	14	-213.12	0.00	
$k = 2$	1.04	108.83	-11.73	23.45	13	-191.67	21.45	1.28E-06
$k = 1$	1.88	97.29	-23.27	46.54	12	-170.58	42.54	7.83E-11

LL Log likelihood, LLmax Maximum log likelihood

Table 3 Stage maturation, duration, and development rates at 20°C, and coefficient α_a calculated for each stage a for $k = 1$

Stage	$\gamma_a(20^\circ\text{C})$	Stage duration time $\bar{d}_a(20^\circ\text{C})$ (days)	Stage development time $\bar{D}_a(20^\circ\text{C})$ (days)	α_a
e	3.64	0.27	-	55.01
n2	2.53	0.40	0.67	134.21
n3	1.05	0.96	1.63	325.81
n4	0.87	1.16	2.78	557.40
n5	0.65	1.53	4.31	864.01
n6	0.81	1.23	5.54	1,110.77
c1	0.54	1.84	7.39	1,479.68
c2	0.58	1.73	9.12	1,827.22
c3	0.60	1.66	10.78	2,159.64
c4	0.40	2.48	13.26	2,656.81
c5	0.29	3.48	16.74	3,353.02
c6	-	4.84	21.57	4,321.76

Fig. 3 Proportion survived at the end of each stage in different temperature regimes fitted to $Sv = \exp(-\phi a^z)$ calculated based on data from Liang and Uye (1997a)

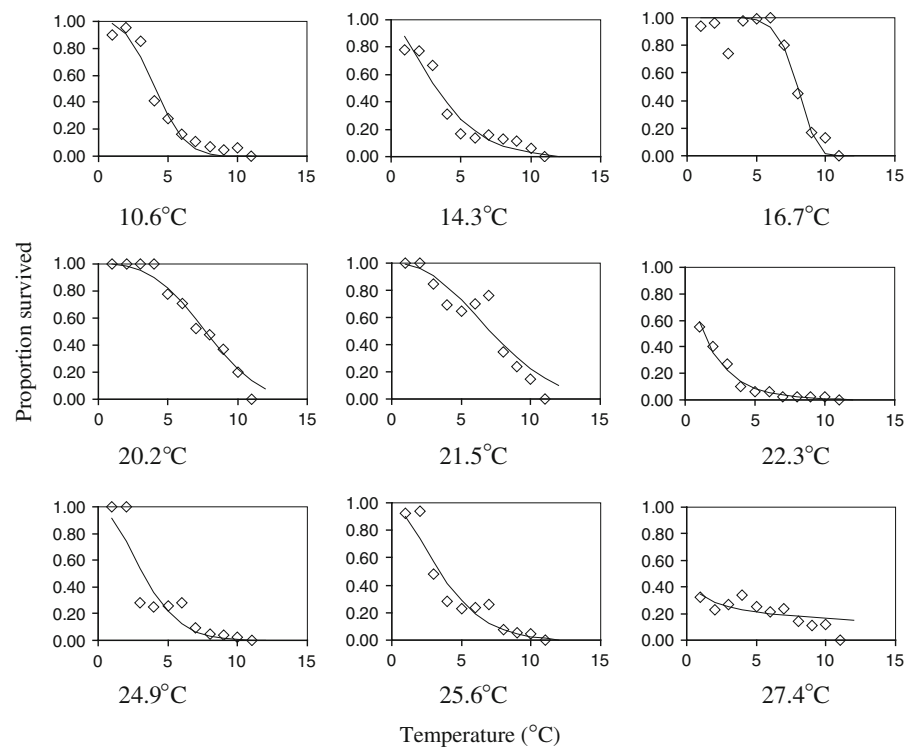


Table 4 Estimation of ϕ and χ in $Sv = \exp(-\phi a^\chi)$ at different temperatures

Temp (°C)	10.60	14.30	16.70	20.20	21.50	22.30	25.60	27.40
ϕ	0.02	0.01	0.00	0.00	0.13	0.53	0.00	0.10
χ	2.69	2.26	7.87	2.93	1.43	0.94	29.24	1.56
RSS	0.05	0.11	0.09	0.02	0.06	0.01	0.09	0.03

RSS Residual sum of squares

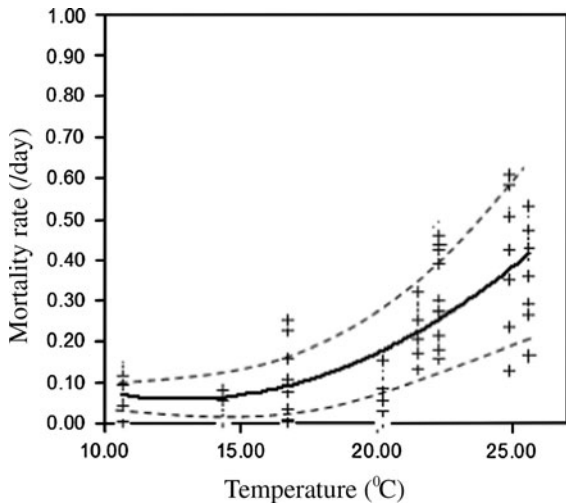


Fig. 4 Quadratic model of daily mortality rates as a function of temperature, estimated for data where all stages are pooled. Parameter values for mortality rate model are $\kappa_2 = 0.0022/\text{day}$, $\kappa_1 = -0.0563/^\circ\text{C day}$, $\kappa_0 = 0.4211/^\circ\text{C}^2 \text{ day}$

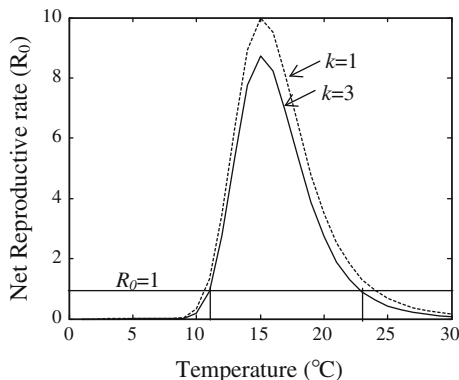


Fig. 5 R_0 plotted as a function of temperature (T) for the cases where $k = 1$ (exponentially distributed stage duration times), and $k = 3$ (gamma distributed stage duration times)

Relatively lower values of $R_0(T)$ for higher k suggest that the fitness of the population is reduced when k is high regardless of the temperature. The model $R_0(T)$ that best fits data was the one with parameter $k = 3$. The uncertainty associated with the estimates

of $R_0(T)$ can not be calculated because parameters taken from the literature did not have confidence estimates (Uye et al. 1983; Liang and Uye 1997a). We found that $R_0 > 1$ between 11 and 23°C, and this is therefore the range within which the habitats are potentially invasible to *P. marinus*. If other conditions in a habitat are ideal and temperature falls within this range, species could grow. At temperatures < 11 and $> 23^\circ\text{C}$, $R_0 < 1$ and habitats with these mean temperatures are non-invasible. If a habitat’s temperature fluctuates seasonally between these two limits, it is tolerable to *P. marinus*.

Application and validation

We mapped the range of habitats where yearly averaged sea surface temperatures is between 11 and 23°C (colored contours in Fig. 6) where they are potentially invasible to *P. marinus*. Hence, the area where there are no contour lines ($23^\circ\text{C} < T < 11^\circ\text{C}$) indicate the habitats where *P. marinus* is non-invasible. Field sampling evidence depicted in Fig. 6 suggests that our predictions fit well into potentially invasible habitat range except for marginal deviations of few occurrences.

Discussion

Here we proposed a novel methodology to model net reproductive rate R_0 , which is a population persistence metric, as a function of temperature (T) for invasive marine copepod *P. marinus* based on the data from experiments. This approach can be generally applied to model R_0 for aquatic copepods that respond to environmental parameters markedly, reproduce year-round, and have multiple overlapping generations (species for e.g. as in Bonnet et al. 2009; Chen et al. 2006). Temperatures giving $R_0(T) > 1$ indicate habitats where the species can physiologically persist, assuming that other environmental factors are suitable for its growth. Temperatures resulting $R_0(T) < 1$

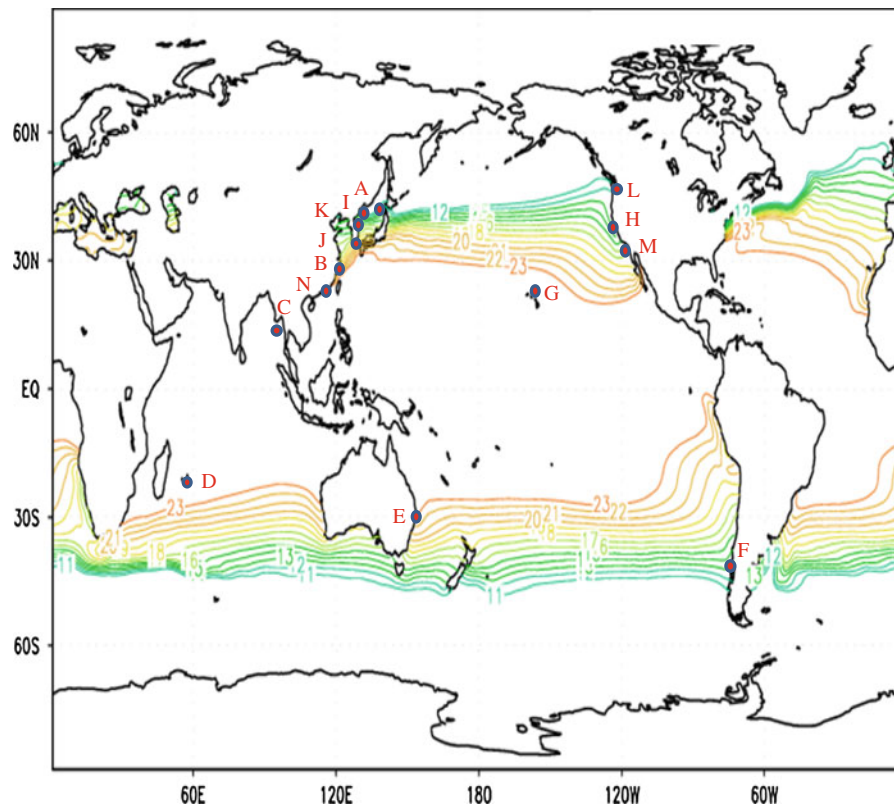


Fig. 6 Contour lines (from 11 to 23°C) depict the range of potentially invisable habitats by *P. marinus* as predicted by our model based on $R_0(T) > 1$ for sea surface temperature (T) data averaged from year 1971–2000 through NOAA interactive database (NOAA Optimum Interpolation (OI) SST V2). Dots are the habitats where *P. marinus* was collected or has established. References are from Fleming and Kramer (1989) except *: (A) West coast of Hokkaido, Japan, Sato (1913), Anraku (1953), Walter (1986); (B) Qing-Chao and Shu-Zhen (1965); (C) Andaman Islands (Pillai 1980); (D) Mauritius (Grindley and Grice

1969); (E) Moreton Bay, Queensland (Greenwood 1977); (F)* Patagonian Waters, Southern Chile (Jones, 1966; Grindley and Grice 1969) from Hirakawa (1986); (G) Oahu, Hawaii (Jones 1966) (Carlton 1985)*; (H)* San Francisco Bay, California (Ruiz et al. 2000); (I) Peter the Great Bay (Brodsky 1948, 1950); (J) Chiba (1956), Tanaka (1966), Tanaka and Huee (1966), Walter (1986b); (K) Brodsky (1948, 1950); (L)* Elliot Bay, Puget Sound, Washington (Cohen 2004), US Geological Surveys; (M) US Geological Surveys; (N) Shen and Lee (1963)

indicate habitats where the species cannot physiologically persist regardless of the other environmental factors. Thus, our approach can conservatively predict habitats which are non-invasible, and thereby habitats which are potentially invisable. Note that we could not calculate confidence intervals in the estimates due to unavailability of primary data.

The habitats that are potentially invisable to *P. marinus* as predicted by our model matched well with field evidence of species occurrences in a global scale except for few marginal deviations (miss-matches) on the borders limiting $R_0(T) = 1$. In particular, we note that from Fig. 6, Elliot bay, Puget Sound is on the border of non-invasibility range limiting $R_0(T)$. It has been recorded in US Geological Surveys that

P. marinus has been sampled in that location by Cohen (2004). However, up to now, there has been any indication that it has established in that location. Further northwards, Piercey et al. (2000) found that there was a large propagule pressure of *P. marinus* on Vancouver harbor (in 25.4% ships sampled, and occurring in densities from 2 to 54 m^{-3}). Our model predicts that Vancouver harbor is also located on the border where $R_0(T) = 1$. We note that in above locations, temperatures fluctuate seasonally throughout the year (DFO Canada). To better predict non-invasibility in such habitats we need a model that incorporates the effect of seasonal variation in temperatures.

Furthermore, had we incorporated the survival data at 27°C, then the upper bound of $R_0(T) = 1$ would have

shifted towards higher temperatures moving the potentially invasible range more towards the tropics. We did not incorporate those data as they were inconsistent with the general trend in mortality rates with respect to increasing temperatures and did not make sense biologically, as outlined in the methods section.

The methodological basis adopted here in determining non-invasible habitats is in contrast to that of ENM (Peterson 2003). ENM predicts habitat-suitability based on a snapshot of environmental conditions and species occurrences (Herborg et al. 2007a; Peterson et al. 2007) by matching the range of environmental variables in native habitats with that in novel habitats (Jeschke and Strayer 2008; Mercado-Silva et al. 2006). For e.g. Genetic Algorithm for Rule-set Prediction (GARP) (Stockwell and Peters 1999) in ENM has been commonly used to predict habitat suitability for both terrestrial and aquatic invasive species (e.g. Herborg et al. 2007a, b; Peterson 2003; Peterson et al. 2007). The above methodology implicitly assumes that the limit to phenotypic plasticity in population fitness traits is exhaustively represented in the observed environmental set in their native habitats. This, in turn, assumes that a species may only survive and reproduce in habitats those having environmental sets similar to that in their native ranges. Often, species tolerate environmental set beyond that is found in native habitats (Lockwood et al. 2006). For example, a species distribution may be confined to a certain native range due to natural barriers rather than environmental parameters (Lonhart 2009) suggesting that absence is not necessarily indicative of a habitat's unsuitability. In such cases, ENM may not be able to fully capture the potential range of the environmental set that a species may tolerate. For this reason, ENM can overlook habitats where a species can potentially survive and reproduce, especially in cases where human-mediated transport may facilitate jump dispersal (e.g. Broennimann et al. 2007). Our approach avoids this particular limitation in ENM.

Our model is designed to quantify R_0 at low introductory populations to determine the species establishment potential. Hence, we did not explicitly account for the density dependence of the population. Further, we disregarded Allee effects (Taylor and Hasting 2005; Courchamp et al. 2008; Kramer et al. 2008) although it may be a factor that acts against species establishment at low population levels (Lockwood et al. 2006; Wittmann et al. 2011). In such cases it

is possible to have a *backward bifurcation*, where a species can persist even when $R_0 < 1$, and hence a different approach would be needed to analyze populations with Allee effects. Biologically, inclusion of the Allee effect may further filter out a subset of non-invasible habitats from potentially invasible habitats. This will complement and further refine our predictions which were made without the case of Allee effect.

Sea surface temperature has been rising over the last few decades (Cane et al. 1997). Our model can be used as a tool to determine how climate change may affect species range expansion. For *P. marinus*, the shape of $R_0(T)$ curve suggests that with increase in sea surface temperature, the potentially invasible habitat range may tend to shift towards currently cooler waters. However, the impact of climate change on current seasonal changes in sea surface temperature may also be a critical factor in determining long term effects on niche shifts. For example, temperature data from Racerock, B.C., spanning the years 1921–2008, indicates that annual low temperatures have not increased as much as annual high temperatures. The impact of such non-linear increases in temperatures may have non-linear effects on R_0 . Hence, we may not be able to rescale the range of R_0 by simply adding the expected increment to mean sea surface temperature.

A proxy of using mean temperatures to characterize a habitat is appropriate in cases where temperature forces R_0 to be either strictly less than 1 or greater than 1 through all seasons. Hence, our result is only applicable to habitats where all seasonal temperatures, were they held constant or averaged, would force $R_0(T)$ to be greater than 1 or less than 1 throughout a year. However, in habitats where temperatures fluctuate seasonally, or daily, forcing $R_0(T) > 1$ in one period, and $R_0(T) < 1$ in another period, we cannot make clear predictions on habitat invasibility by metric $R_0(T)$ alone. Yet, we could presume that a habitat to be more unfavorable to a species when the seasonal fluctuations of a factor forces $R_0 < 1$ in longer period of the year, and vice versa. It may be useful to incorporate the effects of short term and seasonal temperature fluctuations on R_0 (see Bacaer 2009; Bacaer and Ouifki 2007; Wesley and Allen 2009).

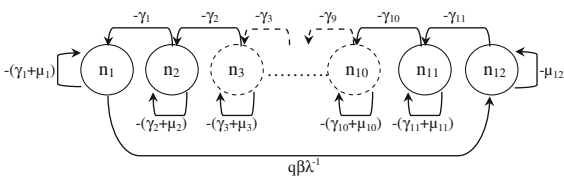
An extension to our model would be to incorporate vital rates as functions of other environmental factors such as salinity. We can then calculate R_0 in a two-dimensional environmental space. It may increase the non-invasible habitat set for the species reducing the potentially

invasive habitat set. Recent work towards modeling the combined effect of temperature and salinity on population persistence is found in Strasser et al. (2011).

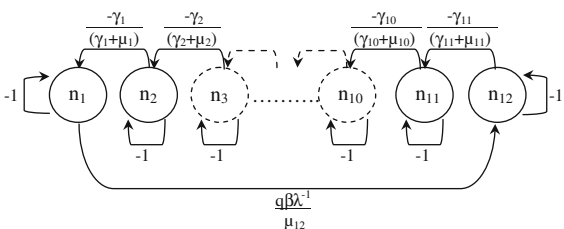
Acknowledgments Financial support for HR and CS came from the NSERC-funded Canadian Aquatic Species Network (CAISN). HR also acknowledges the Department of Biological Sciences, University of Alberta for providing financial support. MAL gratefully acknowledges an NSERC Discovery Grant and a Canada Research Chair. The authors thank Alex Potapov at the Centre for Mathematical Biology, University of Alberta, and Claudio DiBacco at the Bedford Institute of Oceanography, Halifax, for valuable suggestions.

Appendix 1: Deriving R_0 from graph theoretic method

Following the method given in de-Camino-Beck and Lewis (2008), here we have a real 12×12 matrix $(F\lambda^{-1} - V) = a_{ij}$ after decomposing matrix A from Eq. 1 into matrices F , fertility, and V , transition. Hence, for matrix $(F\lambda^{-1} - V)$, there corresponds a labeled directed graph, $D(F\lambda^{-1} - V)$, with nodes 1, 2, ..., 12, and a directed edge (arc) $j \rightarrow i$. The weight of this arc is a_{ij} , and $D(F\lambda^{-1} - V)$ has a loop at node i of weight a_{ii} if $a_{ij} \neq 0$. Thus, we can draw the diagraph, $D(F\lambda^{-1} - V)$, as follows.



We created trivial nodes using graph reduction Rule 1 in de-Camino-Beck and Lewis (2008) by reducing the loops $-a_{ii} < 0$ to -1 at node i 's, for every arc entering i divided by weight a_{ii} . Thus the diagraph will be reduced to the following.



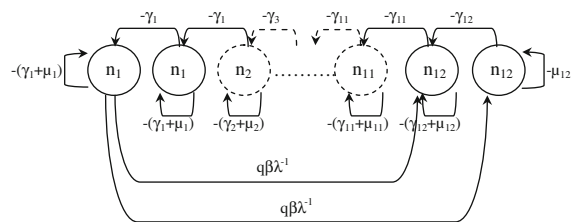
Using Rule 2 in de-Camino-Beck and Lewis (2008), by eliminating arcs through trivial nodes, here we replaced two arcs at a time by $j \rightarrow k$ with weights equal to the product of weights on arc $j \rightarrow i$ and $i \rightarrow k$, for trivial nodes i on a path $j \rightarrow i \rightarrow k$. Thus, it finally yields the following diagraph with a single node.

$$-1 + \frac{q\beta}{\mu_{12}} \prod_{i=1}^{11} \left(\frac{\gamma_i}{\gamma_i + \mu_i} \right) \lambda^{-1}$$

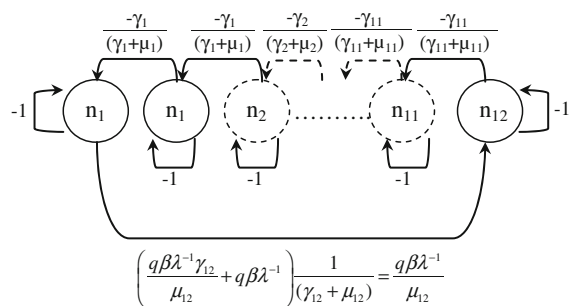
Finally, we set the weight of this loop to zero giving and equation of lambda. The smallest positive roots of this equation yielded R_0 .

$$R_0 = \frac{q\beta}{\mu_{12}} \prod_{i=1}^{11} \left(\frac{\gamma_i}{\gamma_i + \mu_i} \right)$$

Furthermore, when there are 2 sub stages in each stage (that is $k = 2$), the initial graph is given as follows:



Using Rule 1, this can be reduced as follows.



It finally yields,

$$-1 + \frac{q\beta}{\mu_{12}} \prod_{i=1}^{11} \left(\frac{\gamma_i}{\gamma_i + \mu_i} \right)^2$$

Thus, $R_0 = \frac{q\beta}{\mu_{12}} \prod_{i=1}^{11} \left(\frac{\gamma_i}{\gamma_i + \mu_i} \right)^2$.

Similarly, for any k sub stages, it yields,

$$R_0 = \frac{q\beta}{\mu_{12}} \prod_{i=1}^{11} \left(\frac{\gamma_i}{\gamma_i + \mu_i} \right)^k.$$

The same result can be easily derived from $R_0 = \rho[FV^{-1}]$ also.

Appendix 2: General solution for $n_a(t)$

We obtained the following general solution for $n_a(t)$, the proportion of individuals in a given stage a at time t in Eq. 1:

$$\begin{aligned} n_a(t) &= \left(\prod_{i=1}^{a-1} \gamma_i \right) (\underline{b}_a \cdot \underline{v}_a) \quad \text{for } a > 1; \\ n_1(t) &= e^{-\sigma_1 t} \gamma_1 \quad \text{for } a = 1; \end{aligned} \tag{5}$$

where, $\sigma_i = (\gamma_i + \mu_i)$ such that $\gamma_i > 0$ and $\mu_i > 0$ for any stage i and $\sigma_{ij} = (\sigma_i - \sigma_j)$, and \underline{b}_a is a row vector of dimension $1 \times (a - 1)$ of the form $\underline{b}_a = \prod_{j=1}^a B_j$, $j = 1, \dots, a$, where, B_j matrices are non-square matrices such that $B_1 = 1$, $B_2 = \sigma_{21}^{-1}$,

$$B_3 = \begin{bmatrix} \sigma_{31}^{-1} & -\sigma_{32}^{-1} \\ \sigma_{41}^{-1} & 0 & \sigma_{43}^{-1} \\ 0 & \sigma_{42}^{-1} & \sigma_{43}^{-1} \end{bmatrix}, \quad B_4 = \begin{bmatrix} \sigma_{51}^{-1} & 0 & 0 & \sigma_{54}^{-1} \\ 0 & \sigma_{52}^{-1} & 0 & \sigma_{54}^{-1} \\ 0 & 0 & \sigma_{53}^{-1} & \sigma_{54}^{-1} \end{bmatrix},$$

and so on. The general formula for B_k ($k \geq 3$) can be written as,

$$B_k = \begin{bmatrix} \sigma_{k1}^{-1} & 0 & : & 0 & 0 & \sigma_{kk-1}^{-1} \\ 0 & \sigma_{k2}^{-1} & : & 0 & 0 & \sigma_{kk-1}^{-1} \\ : & : & : & : & : & : \\ 0 & 0 & : & \sigma_{kk-3}^{-1} & 0 & \sigma_{kk-1}^{-1} \\ 0 & 0 & : & 0 & \sigma_{kk-2}^{-1} & \sigma_{kk-1}^{-1} \end{bmatrix}_{(k-2) \times (k-1)}$$

Note that due to the dimensions of the B_j matrices, the product $\underline{b}_a = \prod_{j=1}^a B_j$ is a vector. We define the vector \underline{v}_a to be a column vector of the form,

$$\underline{v}_a = \begin{bmatrix} e^{-\sigma_1 t} - e^{-\sigma_a t} \\ e^{-\sigma_2 t} - e^{-\sigma_a t} \\ e^{-\sigma_3 t} - e^{-\sigma_a t} \\ : \\ e^{-\sigma_{a-1} t} - e^{-\sigma_a t} \end{bmatrix}_{(a-1) \times 1}.$$

Appendix 3: Analysis of the case with constant mortality amongst stages

To see that the assumption of equal mortality at each stage cased the mortality rates in Eq. 5 to cancel out

mathematically, consider the case where each μ_i is a constant μ in our solution Eq. 5. Then note that in Eq. 5, σ_{ij} becomes independent of μ , and as a result \underline{b}_a also becomes independent of μ . Further, in \underline{v}_a , $(e^{-\sigma_i t} - e^{-\sigma_a t})$ can be written as $e^{-\mu t} (e^{-\gamma_i t} - e^{-\gamma_a t})$ for each element i . Thus, in the dot product $(\underline{b}_a \cdot \underline{v}_a)$ in the Eq. 5, the term $e^{-\mu t}$ can be separated out as a multiplier, and after redefining, $n_a(t) = e^{-\mu t} \left(\prod_{i=1}^{a-1} \gamma_i \right) (\bar{\underline{b}}_a \cdot \bar{\underline{v}}_a)$, such that term $\left(\prod_{i=1}^{a-1} \gamma_i \right) (\bar{\underline{b}}_a \cdot \bar{\underline{v}}_a)$ becomes independent of μ . i.e. $\bar{\underline{b}}_a = \underline{b}_a$ and $\bar{\underline{v}}_a = \underline{v}_a$ for the special case where $\mu_i = 0$ for all stages i . Now, we can write the proportion of each stage a that remains at time t , $z_a(t)$, with respect to the total population at t :

$$\begin{aligned} z_a(t) &= n_a(t) / \sum_{i=1}^s n_i(t) \\ &= \left(\prod_{i=1}^{a-1} \gamma_i \right) (\bar{\underline{b}}_a \cdot \bar{\underline{v}}_a) / \sum_{j=1}^s \left(\prod_{i=1}^{j-1} \gamma_i \right) (\bar{\underline{b}}_j \cdot \bar{\underline{v}}_j) \end{aligned}$$

where, s is number of stages. Thus, this equation is independent of μ . The numerator of this equation is $n_a(t)$ for the case where $\mu_i = 0$ for all stages for any t . The denominator is the solution to $\sum_{i=1}^s n_i(t)$ for the special case where $\mu_i = 0$ for all stages at any t if the population starts from 1 egg, thus remains 1 at any t . Hence, this can be simplified, so that,

$$z_a(t) = \left(\prod_{i=1}^{a-1} \gamma_i \right) \bar{\underline{b}}_a \cdot \bar{\underline{v}}_a \tag{6}$$

which, is equivalent to $z_a(t) = n_a(t)$ when $\mu_i = 0$ for all stages at any t . Therefore, $z_a(t)$ can be equated with the stage sizes normalized at each time step t in experimental data found in the literature which makes the assumption that $\mu_i = \mu$ for all $i = 1$ to s .

Appendix 4: Fitting Eq. 2 to data using multiple substages

To derive solution to the modified system of equations in Eq. 1 by adding k sub-stages to each stage required using Laplace transformations. It yielded a complicated analytical result. Instead, we modified Eq. 2 to include sub-stages within stages, by assuming small differences in maturation rates among sub-stages. However, the solution in Eq. 2 cannot be simply transformed into a general case for the system to have

multiple sub-stages, because in such case the denominator of the solution in Eq. 2 becomes zero, mathematically, as $\sigma_{ij} = 0$ when i and j were redefined for sub-stages in each stage, such that $\sigma_i = \sigma_j$. Therefore, we implemented the sub-stages for a given stage a by adding and subtracting a small constant (ε) to γ_a such that $\varepsilon \ll \gamma_a$. For example, separating γ_a into three sub-stages would involve splitting γ_a among the three sub-stages, such that maturation rates were $\gamma_a = > [\gamma_a - \varepsilon, \gamma_a, \gamma_a + \varepsilon]$. Then we estimated γ_a using the modified Eq. 2 fitting to data from Uye et al. (1983) for small values of ε .

References

- Ackleha AS, de Leenheer P (2008) Discrete three-stage population model: persistence and global stability results. *J Biol Dyn* 2(4):415–427
- Anraku M (1953) Seasonal distribution of pelagic copepods at Oshoro Bay, west coast of Hokkaido. *Bull Fac Fish Hokkaido Univ* 3:172–192
- Bacaer N (2009) Periodic matrix population models: growth rate, basic reproductive number, and entropy. *Bull Math Biol* 71:1781–1792
- Bacaer N, Ouifki R (2007) Growth rate and basic reproduction number for population models with a simple periodic factor. *Math Biosci* 210:647–658
- Boldin B (2006) Introducing a population into a steady community: the critical case, the centre manifold and the direction of bifurcation. *SIAM J Appl Math* 66(A):1424–1453
- Bolens SM, Cordell JR, Avent S, Hooff R (2002) Zooplankton invasions: a brief review, plus two case studies from the northeast Pacific Ocean. *Hydrobiologia* 480(1–3):87–110
- Bonnet D, Harris RP, Yebra L, Guilhaumon F, Conway DVP, Hirst AG (2009) Temperature effects on *Calanus helgolandicus* (copepoda: calanoida) development time and egg production. *J Plankton Res* 31(1):31–44
- Breteler WCMK, Schogt N, van der Meer J (1994) The duration of copepod life stages estimated from stage-frequency data. *J Plankton Res* 16(8):1039–1057
- Brodsky KA (1948) Free-living copepoda from the Sea of Japan. *Rep Pacif Ocean Inst Fish Oceanogr Vladivostok* 26:3–130. (in Russian)
- Brodsky KA (1950) Calanoida of the far eastern seas and polar basin of the USSR. Keys to the fauna of the USSR. [English transl] Zoological Institute of the Academy of Sciences of the USSR, Moscow (Ref. No. 35) [Israel Program for Scientific Translations, Jerusalem 1967: IPST Catalogue No. 1884]
- Broennimann O, Treier UA, Muller-Scharer H, Thuiller W, Peterson AT, Guisan A (2007) Evidence of climatic niche shift during biological invasion. *Ecol Lett* 10:701–709
- Cane MA, Clement AC, Kaplan A, Kushnir Y, Pozdnyakov D, Seager R, Zebiak SE, Murtugudde R (1997) Twentieth-century sea surface temperature trends. *Science* 275(5302):957–960
- Carlton JT (1985) Trans-oceanic and interoceanic dispersal of coastal marine organisms—the biology of ballast water. *Oceanogr Mar Biol* 23:313–371
- Chen Q, Sheng J, Lin Q, Gao Y, Lv J (2006) Effect of salinity on reproduction and survival of the copepod. *Pseudodiaptomus annandalei* Sewell, 1919. *Aquaculture* 258:575–582
- Chiba T (1956) Studies on the development and systematics of copepoda. *J Shimonoseki Coll Fish* 6:1–90 (in Japanese)
- Cohen AN (2004) An exotic species detection program for Puget Sound. In United states Geological Surveys, p 52. <http://nas.er.usgs.gov/queries/SpecimenViewer.aspx?SpecimenID=161281>
- Cordell JR, Bollens SM, Draheim R, Sytsma M (2008) Asian copepods on the move: recent invasions in the Columbia-Snake River system. *ICES J Mar Sci* 65(5):753–758
- Courchamp F, Berec L, Gascoigne J (2008) Allee effects in ecology and conservation. Oxford University Press, Oxford, p 220
- Cox DR (1967) Renewal theory. Science Paperbacks and Methuen & Co. Ltd., London, p 142
- de-Camino-Beck T, Lewis MA (2007) A new method for calculating net reproductive rate from graph reduction with applications to the control of invasive species. *Bull Math Biol* 69:1341–1354
- de-Camino-Beck T, Lewis M (2008) On net reproductive rate and the timing of reproductive output. *Am Nat* 172(1):128–139
- DFO Canada, BC lighthouse sea surface temperature data. <http://www.pac.dfo-mpo.gc.ca/science/oceans/data-donnees/lighthouses-phares/index-eng.htm>
- Elith J, Leathwick JR (2009) Species distribution models: ecological explanation and prediction across space and time. *Annu Rev Ecol Evol Syst* 40:677–697
- Fleminger A, Kramer SH (1989) Recent introduction of an Asian estuarine copepod, *Pseudodiaptomus marinus* (Copepods: Calanoida), into southern California River Estuary. *J Crustac Biol* 12:260–541
- Greenwood JG (1977) Calanoid copepods of Moreton Bay (Queensland) II. Families Calocalanidae to Centropagidae. *Proc R Soc Qd* 88:49–67
- Grindley JR, Grice GD (1969) A redescription of *Pseudodiaptomus marinus* Sato (Copepoda, Calanoida) and its occurrence at the island of Mauritius. *Crustaceana* 16:125–134
- Herborg L, Jerde CL, Lodge DM, Ruiz GM, MacIsaac HJ (2007a) Predicting invasion risk using measures of introduction effort and environmental niche models. *Ecol Appl* 17(3):663–674
- Herborg L, Mandrak N, Cudmore B, MacIsaac H (2007b) Comparative distribution and invasion risk of snakehead (*Channidae*) and Asian carp (*Cyprinidae*) species in North America. *Can J Fish Aquat Sci* 64:1723–1735
- Hirakawa K (1986) New record of the planktonic copepod *Centropages abdominalis* (copepoda, calanoida) from Patagonian waters, southern Chile. *Crustaceana* 51(3):296–299
- Hurford A, Cownden D, Day T (2010) Next-generation tools for evolutionary invasion analyses. *J Royal Soc Interface* 7(45):561–571

- Jeschke JM, Strayer DL (2008) Usefulness of bioclimatic models for studying climate change and invasive species. *Ann NY Acad Sci* 1134:1–24
- Jiménez-Pérez JL, Castro-Longoria E (2006) Range extension and establishment of a breeding population of the asiatic copepod, *Pseudodiaptomus marinus* Sato, 1913 (calanoida, Pseudodiaptomidae) in Todos Santos bay, Baja California, Mexico. *Crustaceana* 79(2):227–234
- Jones EC (1966) A new record of *Pseudodiaptomus marinus* Sato (Copepoda, Calanoida) from brackish waters of Hawaii. *Crustaceana* 10:316–317
- Kramer AM, Sarnelle O, Knapp RA (2008) Allee effect limits colonization success of sexually reproducing zooplankton. *Ecology* 89(10):2760–2769
- Lee HW, Ban S, Ikeda T, Matsuishi T (2003) Effect of temperature on development, growth and reproduction in the marine copepod *Pseudocalanus newmani* at satiating food condition. *J Plankton Res* 25(3):261–271
- Liang D, Uye S (1997a) Population dynamics and production of the planktonic copepods in a eutrophic inlet of the island Sea of Japan. IV. *Pseudodiaptomus marinus*, the egg-carrying calanoid. *Mar Biol* 128(3):415–421
- Liang D, Uye S (1997b) Seasonal reproductive biology of the egg-carrying calanoid copepod *Pseudodiaptomus marinus* in a eutrophic inlet of the island of Japan. *Mar Biol* 128(3):409–414
- Lockwood J, Hoopes M, Marchetti M (2006) *Invasion ecology*. Wiley Blackwell, Oxford, p 312
- Lonhart SI (2009) Natural and climate change mediated invasions. In: Crooks JA, Rilov G (eds) *Biological invasions in marine ecosystems: ecological, management, and geographic perspective*. Springer, Berlin, pp 57–76
- MacDonald N (1978) *Time lags in biological models*. Springer, Berlin, p 112
- Mercado-Silva N, Olden JD, Maxted JT, Hrabik TR, Vander Zanden MJ (2006) Forecasting the spread of invasive rainbow smelt in the Laurentian Great Lakes region of North America. *Conserv Biol* 20(6):1740–1749
- NOAA Optimum Interpolation (OI) SST V2. <http://www.esrl.noaa.gov/psd/data/gridded/data.noaa.oisst.v2.html>
- Peterson AT (2003) Predicting the geography of species' invasions via ecological niche modeling. *Q Rev Biol* 78(4):419–433
- Peterson AT, Williams R, Chen G (2007) Modeled global invasive potential of Asian gypsy moths, *Lymantria dispar*. *Entomol Exp Appl* 125(1):39–44
- Piercey GE, Levings CD, Elfert M, Galbraith M, Waters R (2000) Invertebrate fauna in ballast water collected in vessels arriving in BC ports, especially those from Western North, Pacific. *Can Data Rep Fish Aquat Sci* 1060:50
- Pillai PP (1980) A review of the calanoid copepod family Pseudodiaptomidae with remarks on the taxonomy and distribution of species from the Indian Ocean. *J Mar Biol Ass India* 18:242–265
- Qing-Chao C, Shu-Zhen Z (1965) The planktonic copepods of the Yellow sea and the east China sea. 1. Calanoida *Studia Mar Sin* 7: 20–131 (Peijing Science Publishers)
- Razouls C, de Bovée F, Kouwenberg J, et Desreumaux N (2011) Diversity and geographic distribution of Marine Planktonic Copepods. <http://copepodes.obs-banyuls.fr/en>
- Ruiz GM, Fofonoff P, Carlton JT, Wonham MJ, Hines AH (2000) Invasion of coastal marine communities in North America: apparent patterns, processes, and biases. *Annu Rev Ecol Evol Syst* 31:481–531
- Sato T (1913) Pelagic copepods (No. 1). *Scient Rep Hokkaido Fish Expl Stn* 1:1–79 (in Japanese)
- Shen C, Lee F (1963) The estuaries of Chiekong and Zaikong Rivers. *Acta Zool Sin* 15:573–596
- Stockwell DRB, Peters DP (1999) The GARP modelling system: problems and solutions to automated spatial prediction. *Int J Geogr Inf Sci* 13:143–158
- Strasser CA, Lewis MA, DiBacco C (2011) A mechanistic model for understanding invasions using the environment as a predictor of population success. *Divers Distrib* 1–15
- Tanaka O (1966) Neritic copepoda, calanoida from the north-west coast of Kyushu. *Proc Symp Crustacea 1965, Ernakulum, Cochin (Ser. 2)* *Mar Biol Ass India* 38–50
- Tanaka O, Hue JS (1966) Preliminary report on the copepoda found in the tidal pool along the north-west coast of Kyushu. *Proc Symp Crustacea 1965, Ernakulum, Cochin (Set. 2)* *Mar Biol Ass India* 57–73
- Taylor CM, Hasting A (2005) Allee effect in biological invasions. *Ecol Lett* 8:895–908
- US Geological Surveys. <http://nas.er.usgs.gov/queries/SpecimenViewer.aspx?SpecimenID=161281>
- Uye S, Iwai Y, Kasahara S (1983) Growth and production of the inshore marine copepod *Pseudodiaptomus marinus* in the central part of the inland Sea of Japan. *Mar Biol* 73:91–98
- van den Driessche P, Watmough J (2002) Reproduction numbers and sub-threshold endemic equilibria for compartmental models of disease transmission. *Math Biosci* 180:29–48
- Venables WN, Ripley BD (2002) *Modern applied statistics with S*, 4th edn. Springer, Berlin, p 495
- Wallinga J, Lipsitch M (2007) How generation intervals shape the relationship between growth rates and reproductive numbers. *Proc Royal Soc Biol Sci* 274(1609):599–604
- Walter TC (1986) The zoogeography of the genus *Pseudodiaptomus* (Calanoida: Pseudodiaptomidae). *Syllogeus* 58:(Nat Mus Can) 502–508
- Weibull W (1951) A statistical distribution function of wide applicability. *J Appl Mech Trans ASME* 18(3):293–297
- Wesley CL, Allen LJS (2009) The basic reproductive number in epidemic models with periodic demographics. *J Biol Dyn* 3(2–3):116–129
- Wittmann MJ, Lewis MA, Young JD, Yan ND (2011) Temperature-dependent Allee effects in a stage-structured model for *Bythotrephes* establishment. *Biol Invasions*. doi: [10.1007/s10530-011-0074-z](https://doi.org/10.1007/s10530-011-0074-z)